New model for structural optimisation of airborne wind energy systems with rotary transmission

To cite this article: Jannis Wacker *et al* 2023 *J. Phys.: Conf. Ser.* **2626** 012011

New model for structural optimisation of airborne wind energy systems with rotary transmission

Jannis Wacker[1,2], Michael McWilliam[1], Michael Muskulus[2] and Mac Gaunaa[1]

[1] Department of Wind Energy, Technical University of Denmark, Frederiksborgvej, 4000 Roskilde, Denmark

[2] Department of Civil and Environmental Engineering, Norwegian University of Science and Technology, Høgskoleringen, 7491 Trondheim, Norway

E-mail: `j.wacker@posteo.de`

Abstract. Rotary Airborne Wind Energy Systems (RAWES) are networks of wings that act as flying wind turbines. The power extracted from the wind can be transmitted to ground-based generators through open tensegrity structures. In recent years, there have been different approaches to the topology of the Tensile Rotary Power Transmission (TRPT) and prototype designs are often driven by trial-and-error. This paper proposes a steady-state model with numerical optimisation to accelerate the development and prototyping of AWES by supporting the evaluation of new design concepts.

The coupled steady state model uses aerodynamics and structural dynamics to analyse the AWES performance. A novelty is, that the model includes both cross-wind pressure drag and axial friction drag acting on the tethers and frames in the tensegrity structure. Validation of the model has been achieved using data from field measurements of two prototypes.

In conclusion, using the proposed optimisation, RAWES with TRPT can be designed to maximise power density, coefficients of performance or power harvesting factor. While RAWES will not be able to outperform conventional wind turbines, they have the potential advantages in niche applications due to reduced costs and simplified logistics resulting from reduced material usage.

1. Introduction

The rapid expansion of wind energy, necessary for a sustainable energy transition, faces significant challenges, including limited wind resources, public acceptance and supply chain issues.

Airborne Wind Energy Systems (AWES) may present a solution for these problems. Good introductions to AWES technology and its related literature can be found in [1, 2] and [3] respectively. In general AWES consist of flying wings that are tethered to the ground, thus making towers of conventional wind turbines obsolete. Thereby AWES can reach higher altitudes with better wind resources, reduce material usage and potentially decrease visual impact.

Within the field of AWES, there are a wide variety of different concepts, the most common being kites harvesting power through a pumping cycle [1]. This article investigates the less common fixed ground station Rotary Airborne Wind Energy Systems (RAWES) with Tensile Rotary Power Transmission (TRPT) where the lift is provided by the rotors autogyro effect and optionally a lifter kite [4, 5] (Figure 1).

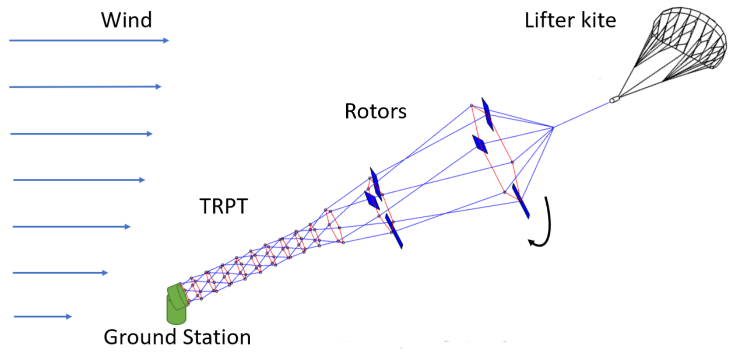

Figure 1. Overview of Daisy Kite as example for RAWES concepts.

A lifter kite (marked black) provides uplift and tension to help maintain a steady operating height and tether tension. The lifter kite does not rotate, in contrast to the rest of the TRPT system. One or more rotors, consisting of airfoil blades (dark blue) attached to a polygon frame (red), convert wind power to mechanical power by inducing a torque to the system. A set of tethers (blue) and rigid frames form the TRPT and transfer the rotational power from the rotors to the ground station (green) like a soft shaft. While the rigid frames can withstand compression loads, the tethers need pretension. The more torque is applied, the higher is the deformation angle between neighbouring frames and the whole tensegrity system becomes shorter. The ratio between applied torque and tension along the rotation axis should not exceed a certain limit, otherwise the tethers between neighbouring frames twist up and fail to transmit any significant power [6, 7]. Meanwhile the rotation of the tensegrity system causes aerodynamic drag opposing the torque from the rotors. Lastly the ground station contains an electric power generator with speed or torque control.

Within this category, several RAWES concepts have been developed, diverging in their take-off and landing strategies as well as in their size and number of blades, tethers and frames [4, 6].

This paper presents a methodology for modelling the steady-state operation of different concepts and optimising the component sizing. This will allow a better comparison between concepts and a faster evaluation of new concept ideas. System dynamics as well as take-off and landing strategies are not part of the analysis.

2. Modelling

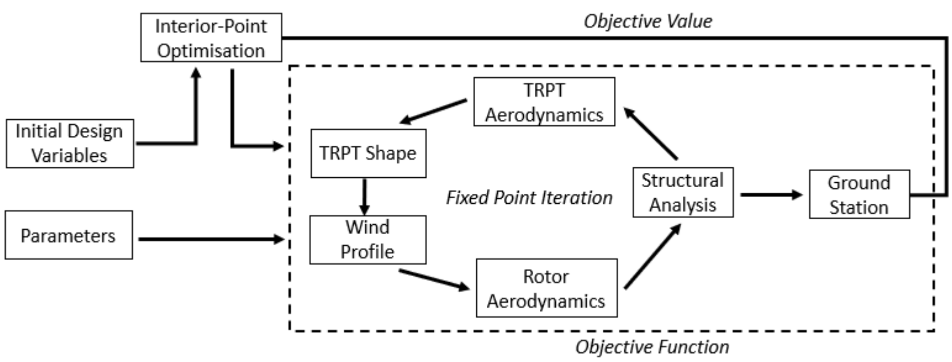

Figure 2. Block diagram of optimisation model.

An overview of the model architecture can be seen in Figure 2. The model is fed a set of parameters describing the RAWES concept features (e.g. the number of tethers and frames in the TRPT sections) and other fixed assumptions (e.g. rated wind speed, corresponding reference

Table 1. List of parameters for concept features and design variables.

	Symbol	Description	Unit
Concept Parameters	n_t	Number of tethers per tensegrity segment	-
	n_f	Number of polygon corners per frame	-
	n_R	Number of polygon frames	-
	n_r	Number of rotors	-
	n_b	Number of blades	-
	v_{ref}	Rated wind speed	m/s
	T_l	Assumed lifter tension	N
	h_{ref}	Reference height for v_{ref}	m
	ψ	Wind shear exponent	-
	ρ	Air density	kg/m^3
Design Variables	$R_{rot}, R_2, \ ..., \ R_{gen}$	TRPT frame radi	m
	$L_{t1}, L_{t2}, \ ..., \ L_{tn}$	TRPT tether length	m
	l_b	Blade length	m
	β	Elevation angle of rotation axis	°
	α	Blade pitch	°
	λ	Tip speed ratio	-

height and air density) as listed in Table 1. Further, a set of Initial Design Variables is defined as input, describing the operating conditions (e.g. tip speed ratio, pitch angle and elevation angle) as well as the TRPT dimensions (e.g. tether lengths, frame radii and blade length).

These design variables are subject to change by Matlab's interior-point optimisation algorithm *fmincon*. The full optimisation problem including the constraints preventing failure in the TRPT can be defined as follows, with a comprehensive explanation given in [8]:

$$
\begin{array}{lll}
\min_{R,L_t,\beta,l_b,\alpha,\lambda} & -P_d & \\
\text{s.t.} & \delta_i < \delta_{c,\ i} & \text{for} \quad L_{t,i} > R_{1,i} + R_{2,i} \ and \ \forall i \in n_R - 1 \\
& \delta_i < \delta_{lim,i} & \text{for} \quad L_{t,i} \leq R_{1,i} + R_{2,i} \ and \ \forall i \in n_R - 1 \\
& R_{rot} + l_b < \sum (L_s) \ \ sin(\beta) + R_{gen} & \\
& R_{rot} \geq \frac{l_b}{2} & \\
& R_{lb} \ < \ R \ < \ R_{ub} & \\
& L_{t,\ lb} \ < \ L_t \ < \ L_{t,\ ub} & \\
& \beta_{lb} \ < \ \beta \ < \ \beta_{ub} & \\
& l_{b,\ lb} \ < \ l_b \ < \ l_{b,\ ub} & \\
& \alpha_{lb} \ < \ \alpha \ < \ \alpha_{ub} & \\
& \lambda_{lb} \ < \ \lambda \ < \ \lambda_{ub} &
\end{array}
$$

The objective value can be set as the systems Power Density defined as $P_d = \frac{P_{out}}{m_{tot}}$, the Coefficient of Performance $C_p = \frac{P_{out}}{P_{swept}}$ or the Power Harvesting Factors $\zeta = \frac{P_{out}}{P_{blade}}$, where P_{out} is the generated electrical Power output, m_{tot} is the total mass of the system, P_{swept} is the potential wind power available within the rotors swept area and P_{blade} is the potential power available in the total blade area. The different objective values were chosen as they set the power output in the context of critical design factors like material cost, space usage and blade size.

The objective function is a full system analysis, performed in several iterative steps.

(i) **TRPT Shape -** The angular deformation of the tensegrity system is determined by its dimensions and the forces acting on it as seen in Figures 3. In the first iteration the force parameters have to be estimated. The resulting angular deformation δ (Figure 4) determines the length of the TRPT segment L_s and thereby the operational height h of the rotor and the TRPT segments.

$$h = \sin\beta \sum_{i=1}^{n_R-1} \sqrt{L_{t,i}^2 - R_{1,i}^2 - R_{2,i}^2 + 2R_{1,i}R_{2,i}\cos\delta_i} \quad (1)$$

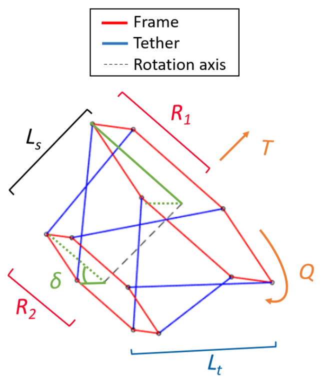

Figure 3. Angular deformation and dimensions of one tensegrity segment.

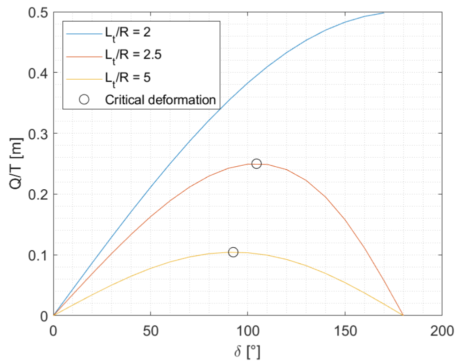

Figure 4. Transmitted force ratio over deformation angle δ in one tensegrity segment.

(ii) **Wind Profile:** Wind speeds are calculated at the rotor and each TRPT segment, depending on their height, following a power law distribution with respect to a given rated wind speed, $v_w = v_{ref}(\frac{z}{z_{ref}})^\psi$

(iii) **Rotor Aerodynamics:** The rotor power and forces are modelled using the BEM analysis of NREL's *AeroDyn* tool [9]. Pitt and Peters tilt correction is used to compensate for the cosine losses due to the rotors tilt angle which is equal to the elevation angle of the rotational axis relative to the ground.

(iv) **Structural Analysis:** A structural model determines the necessary cross-sectional area A and diameter d of the tether and frame components within the tensegrity system, based on static analysis with additional safety factor SF to avoid structural failure due to the axial forces F_{axial} though centrifugal forces as well as buckling effects are not included.

$$A = \frac{F_{axial}}{\sigma} SF \quad (2)$$

The system dimensions are further used to calculate the mass of the lifter kite, rotor, TRPT and ground station. The sum of these is the total mass m_{tot}.

(v) **TRPT Aerodynamics:** Tulloch developed a procedure to calculate the aerodynamic resistance of the TRPT tethers $P_{loss,t}$, considering their viscous and pressure drag C_{vd} and C_{pd} due to their relative wind speed [6]. In this model, Tulloch's procedure was adapted to additionally identify the power loss due to the drag acting on the frame components $P_{loss,f}$.

$$P_{loss,f} = n_f \frac{1}{2\pi} \int_0^{l_f} \int_0^{2\pi} \omega R_{fp} \rho v_w^2 l_{fp} d_f \pi n_f C_{pd_f} \left(\frac{\omega R_{fp}}{v_w} + sin(\theta_i) cos(\beta) \right)^2 d\theta_i dl_{fp} \quad (3)$$

The full derivation of Equation 3 can be found in Wacker's master thesis [8].

(vi) **Ground Station:** If the calculated forces from the rotor and TRPT aerodynamics show a sufficiently small change compared to the previous iteration, such that $\Delta F < 0.1N$, the resulting torque and rotational speed are converted into the electric power output under consideration of a predetermined generator efficiency, $P_{out} = (P_{rot} - P_{loss,f} - P_{loss,t})\ \eta_{gen}$. This is then used to return the objective value to the optimiser.

3. Parameter study

The design variables of interest are the shape and dimensions of the tensegrity system, as well as the rotational speed and pitch angle of the rotor blades. A parameter study was carried out over these variables to evaluate different trends for successful designs and concepts.

The parametric analysis investigated the impact of several parameters and design variables on the power performance with respect to the Daisy Kite base case. It was shown in [8] that for the given wind shear profile and the Daisy Kite length an angle of 23° yields the highest output, however, this might change depending on the system size and shear exponent. When compared to the same rotor without yaw, the cosine losses amount for 8% of the potential energy in the wind.

One of the more interesting results is that tensegrity systems with double-helix design (where $n_t = n_f = 2$) have a significant reduction in drag losses compared to TRPT designs with increasing number of tethers and polygon sides, as seen in Figure 5, but comes at the cost of operational stability, because turbulence in the wind can disturb the tethers pretension, causing entanglement.

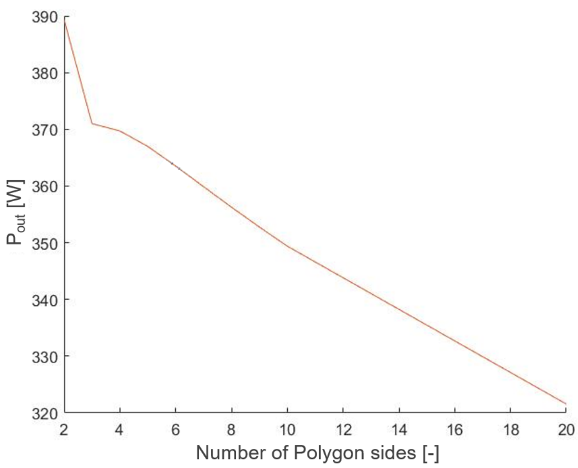

Figure 5. Power output over number of tethers and frame corners.

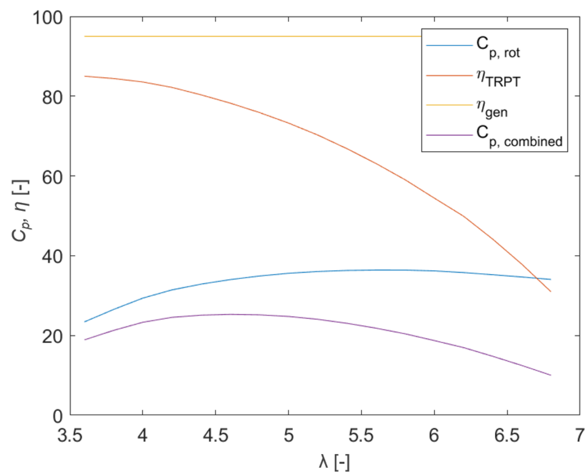

Figure 6. Power transformation and transfer efficiencies over tip speed ratio.

Another result, seen in Figure 6, shows the impact of the 3-bladed rotors tip speed ratio λ on the rotors coefficient of performance $C_{p,rot}$, the TRPT efficiency η_{TRPT}, the generators efficiency η_{gen} as well as the combined coefficient of performance $C_p = C_{p,rot}\eta_{TRPT}\eta_{gen}$. The drag losses in the tensegrity system are proportional to ω^3, therefore η_{TRPT} decreases rapidly. $C_{p,\ rot}$ however peaks around $\lambda = 6$, such that the resulting combined C_p peaks around 4.5.

4. Results

As the following sections will show, the numerical model of the objective function has been validated against experimental data from the Daisy Kite by Windswept and Interesting [4] and MAR1 prototype by SomeAWE Labs [10]. Then some optimisation studies were conducted to see how these designs could be improved.

4.1. Daisy Kite

Figure 7 shows a Daisy Kite prototype in operation. During field tests of the modelled Daisy Kite, with TRPT version 4 and 3 rigid rotors at $\lambda = 5$, the power output was measured around 150W, with a large standard deviation of 70W [6]. The corresponding wind speed was $5.3m/s$ measured at $5m$ height with a standard deviation around $1.1m/s$. Unfortunately these conditions do not allow for a precise comparison. But the experimental results indicate that the model, with power output of 164W and an estimated error of 9%, is within the reasonable range.

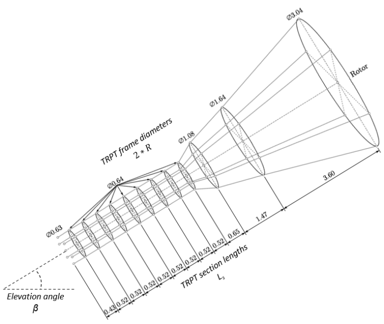

Figure 7. Sketch of Daisy Kite dimension for TRPT Version 4 prototype [6].

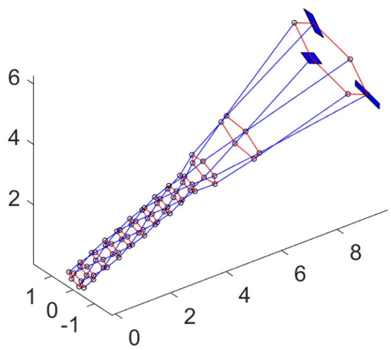

Figure 8. Daisy Kite base-case Model with $P_d = 16.1W/kg$.

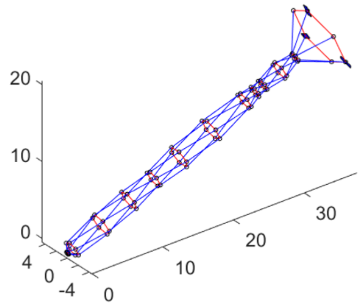

Figure 9. Optimised Daisy design with TRPT shape for maximum power density of $P_d = 52W/kg$

The results for the model in Figure 8 can also be compared to Tulloch's simplified steady-state model. A good metric for comparison is the power transmission efficiency which was reported by Tulloch as $\eta_{TRPT} = 88.6\%$ and obtained here as $\eta_{TRPT} = 73.0\%$. This decrease in efficiency is expected, as the tether drag accuracy was improved and the frame drag was newly implemented. For this particular TRPT shape $P_{loss,\ f} \approx \frac{P_{loss,\ t}}{2}$.

When running the optimisation of the Daisy kite base case, the solver encountered the problem that the objective function with respect to the 29 design variables exhibited several local minima. The problem could have been tackled with different optimisation algorithms or normalised design variables. However there was a pattern found in several local minima, which hold some lessons about the limitation of this design.

Given the dimension of the Daisy Kite base case, Figure 9 shows the optimisation result after 27 iterations with 360 function calls with an optimality value of $7.3 \cdot 10^{-10}$. Besides these statistics hinting towards a successful optimisation, the result is only a local minima. It seems like the solver increases the frame radii to reach higher altitudes. However it is unclear why the frame below the rotor is so slim. One theory is, that the weight contribution of the rotor, lifter and ground station are so much larger, that the additional frame mass due to high forces is not very important.

Compared to the base case, the power density increased by a factor of 3.2 while the power output was increased by a factor of 7.6. So the design was certainly improved although not in an intuitive way.

4.2. MAR1

SomeAWE Labs' MAR1 design, as seen in Figure 10 uses $0.5m$ long rods as frames, crosswise connected by $0.5m$ long tethers. With a total of 80 TRPT segments, the system is longer than the Daisy Kite prototypes. A test at $10m/s$ wind speed with a tip speed ratio of 3.2 resulted in a power output of $364W$ or $C_p = 0.1$ [10].

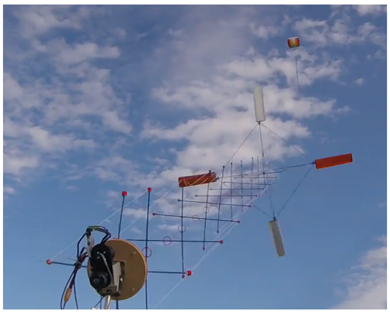

Figure 10. Picture of MAR1 prototype [10].

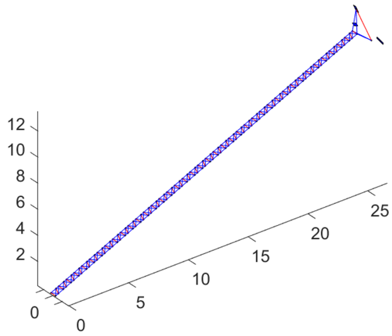

Figure 11. MAR1 base-case model with $P_d = 45W/kg$.

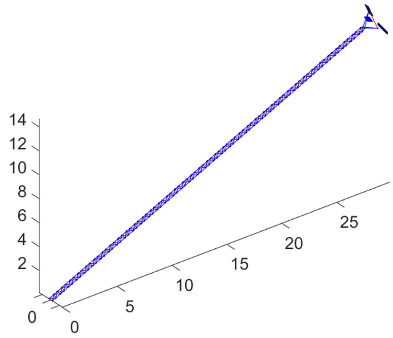

Figure 12. Optimised MAR1 design with $P_d = 85W/kg$

When applying the MAR1 dimensions and operating conditions to the steady state system, a power output of $337W$ is obtained, suggesting $C_p = 0.1$ and the error of this model compared to the measured data is 7.4%.

However, the AeroDyn tool limits the the number of blades in the model to 3 blades per rotor, while the MAR1 prototype uses 4. Rotors with more blades have a lower tip speed ratio λ, so λ of the 3-bladed MAR1 model was optimised to 4.19, resulting in a power output of $393W$, with $C_p = 0.12$ and $P_d = 45W/kg$. The error compared to the measured data is 7.97%, which might be due to inaccurate wind measurements, or simplifications made in the model. For example, the prototypes frame joint shape and details of the rotor frame are neglected in the model. The optimisation result yielded first order optimality values in the range of 10^{-10}, giving some confidence in the success of the optimisation. When repeating the optimisations with different initial conditions, the same result was achieved, suggesting that the solution is a global minimum. The frame radii of the result are very close to its lower bound of 0.1 m, forming a long and slim TRPT. as seen in Figure 12.

4.3. The Pyramid
The Pyramid concept developed by Read, Tveide and Tulloch [11] uses only one TRPT segment with triangular frames. The concept is not tested yet, but the physical limitations can be described by the critical force ratio of the TRPT, which was plotted in Figure 4.

The Pyramid has only one TRPT segment, three tethers and no lifter kite. First, the Pyramid design is optimised with respect to power density P_d.

The optimised design seen in Figure 13 reaches $12.4kW$ power output with $4.3m$ long blades, an average rotor radius of $20m$, $45m$ long tethers, and a ground station that is at least $6m$ high. With $\lambda = 4.88$, the rotor's speed is greater than the optimum efficiency of the Daisy design, because the drag contribution from the TRPT is smaller and the tip radius is much bigger. This trend can also be seen in conventional wind turbines.

When the objective value in the optimisation problem is changed to the systems coefficient of performance C_p, the resulting design keeps similar tether length and frame radii as in Figure 13, but reaches the upper blade length limit of 10 m and has a power output of 57.4 kW. The increased C_p of 0.25 comes at the cost of a significantly reduced power density and power harvesting factor.

Despite having a 10m large (and therefore heavy) tower as ground station (Figure 14), the systems mass is dominated by the rotor. This suggests that lightweight hallow carbon composite blades will outperform foam blades which are used for most prototypes.

The last optimisation was made with the power harvesting factor ζ as objective value. The resulting system (Figure 15) has a maximised ζ of 5.4, producing 22.7 kW with blades of 5.2 m

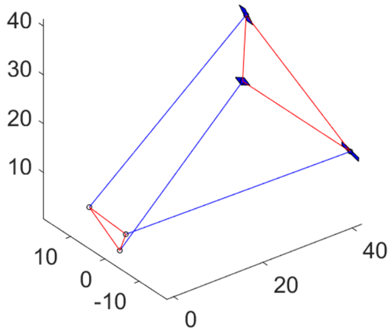

Figure 13. Optimisation results for the Pyramid design with objective value P_d.

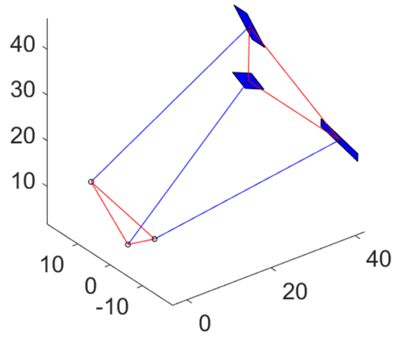

Figure 14. Optimisation results for the Pyramid design with objective value C_p.

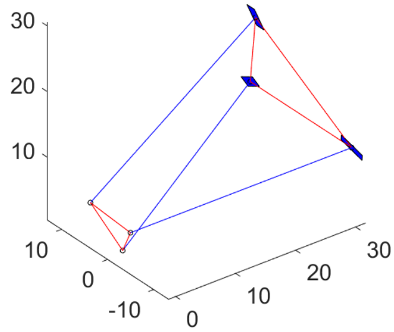

Figure 15. Optimisation results for the Pyramid design with objective value ζ.

length. The power density is fairly high at 35 W/kg. The coefficient of performance is 0.16.

4.4. Summary

A summary of the Base Cases and the optimisation results is given in Table 2. All listed results are based on the same wind profile and are thus comparable.

Table 2. Summary of Optimisation Results

Concept	Objective Value	P_{out}	P_d	ζ	$C_{p,comb}$	$C_{p,rotor}$	η_{TRPT}
Daisy	base-case	168	16.1	3.31	0.23	0.3	0.79
Daisy	P_d	1282	52	4.8	0.18	0.27	0.68
MAR1	P_d	405	85	2.66	0.23	0.29	0.84
Pyramid	P_d	11993	40	5.3	0.12	0.19	0.65
Pyramid	C_p	57443	18.62	4.2	0.25	0.31	0.84
Pyramid	ζ	22716	35	5.4	0.16	0.23	0.73

As reference, the highest measured power harvesting factor ever was $\zeta = 8$ [2] for the Makani design, which used a large wing with onboard generation. Large conventional wind turbines have reached $C_p = 0.52$ and an approximate $\zeta = 5.5$ [2]. Therefore the prototypes as well as the optimised design perform worse than Makani power or conventional wind turbines when using these metrics.

5. Discussion

It was shown, that with little adjustments, the proposed model can analyse, optimise and compare different RAWES concepts and designs. This could be used to improve existing prototypes, or analyse completely new concepts.

A parameter study was made to identify benefits of different operating conditions and concept features. However, the theoretical considerations must still be supplemented with practical aspects like stability as well as take-off and landing procedures.

It is not possible to determine an overall best RAWES design or concept, as this would depend greatly on the specific set of operating conditions. However, the analytical expressions 1, 3 and 2 for height, tether drag and structural analysis suggest three key design principles to maximise power output while minimising weight:

- Increase the rotors swept area and thereby the harvested power. This is achieved primarily by increasing the rotor radius, but also by increasing the blade length.
- Keep the frame radii R small in order to reduce the TRPT drag $P_{loss} \propto R^3$ and the size of the ground station.
- Streamline the frame radii and tether lengths of subsequent TRPT segments. This reduces the forces in tethers and frames and thereby their required weight.

It was therefore surprising to see the first optimisation find solutions that do not follow these principles. The risk of finding local minima is a weakness of the current model.

When scaled by a factor k, the power output of RAWES increases proportional to their area, as well as the wind speed cubed, which increases with respect to the shear exponent such that $P_{out} \propto k^{2+3\psi}$. Mass however increases proportional to the cube of the scaling factor $m \propto k^3$. It is therefore to be expected, that the optimisation with respect to the power density $P_d = \frac{P_{out}}{m_{tot}}$ is biased towards smaller models.

The fact that the dimensions of the optimisation results do not tend towards zero, is due to the lifter weight and minimum mass of the components (due to the lower bounds of the design values) forming a minimum system mass, similar to fixed costs. As the optimisations indicate, the optimised designs increase their power production through higher elevation and bigger rotor radii, before this growth is limited by the rapidly increasing blade mass.

Optimisations can be a very effective tool for identifying high performance design configurations for RAWES. The optimisation should however never be the only design criteria as it is based on various assumptions and limitations. Most importantly, the assumption of steady state, with the TRPT and rotor being in a static equilibrium. This assumption neglects dynamic effects like turbulent wind and internal vibrations. The increased stress due to such dynamic effects is compensated in the steady-state model by applying a safety factor to the cross-sectional areas of tethers and frames (Equation 2). However, the steady state model cannot detect if a certain operating point is unstable due to dynamic effects and assumes constant rotational speed and elevation angle throughout the system. When modelling the TRPT as a multi spring disc model, Tulloch found that the internal vibrations are not insignificant. The TRPT stiffness for example causes a positive feedback loop in response to fluctuations in the wind, potentially leading to resonance [5].

The TRPT frames are assumed to rotate in parallel planes with a common axis of rotation. In practice, the weight of its components causes the TRPT network to form a catenary shape. This can create cyclic slack in the rotating tethers, increase fatigue and will effect the final elevation angle of the rotor [6]. The effect is stronger for long TRPT networks and can be minimised through lightweight materials and high axial tension.

It is common that prototypes are build at different scales and tested at different wind conditions, so the power output alone is not a good comparison. Metrics for the efficiency like the Power Harvesting Factor ζ or the coefficient of performance C_p provide useful information, can however not show at what cost this efficiency is achieved. For that, the LCOE would be the best metric, but the necessary data is location dependant and often not available during early development phases.

For a reasonable comparison, different concepts have to be optimised for the same set of external conditions and evaluated based on their resulting power density. Table 2 shows a list of different optimisations and their results, given the same wind shear profile. It is difficult to identify a clear correlations between the metrics for power output, power density, coefficient of performance and power harvesting factor.

In terms of power density and combined efficiency, the optimised MAR1 design outperforms the other results, except the pyramid design that was specifically optimised with respect to C_p. The designs do not perform as well as conventional turbines. However, looking at the power output and efficiencies might not always be a fair comparison. A modern 2 MW turbine has blades that weight around 11.3 tons resulting in a power density of 60 W/kg, without even counting the nacelle, tower and foundations. It is shown here, that optimised RAWES can perform in the range of 40 to 85W/kg despite considering the total system weight. Assuming the ground station and nacelle scale equally with power, RAWES would allow material savings corresponding to the weight of conventional turbine towers and their foundation.

6. Conclusions

In conclusion, the proposed steady-state model and optimisation can be a useful tool to find the best structural design for different RAWES concepts at specific rated wind conditions. Depending on the preference, the optimisation can be used to maximise the systems power density, coefficient of performance, or power harvesting factor. In the best case scenario, all three metric could be used to quickly evaluate new ideas, or to rate the potential of different concepts.

7. Further Work

Further work on this model could improve the rotor efficiency by including different degrees of twist along the blade and by including control schemes, like cyclic pitch as done by someAWE Labs [11].

For open center rotors with relatively small wings compared to the tip radius the Prandtl model does not perform very well [12]. New approaches, like Shen's tip loss model have a lot of potential and should be further validated in combination with yaw correction.

In general, the dynamic analysis of AWES in turbulent flow poses a major gap in current research. This includes both time marching results along with eigen frequency analysis to assess stability.

Author Contributions

This work came out of a MSc project where Jannis Wacker was the student. Jannis Wacker constructed the model, acquired the results and made significant contributions to the interpretations of the data. Michael McWilliam, Michael Muskulus and Mac Gaunaa made substantial contributions to the conception or design of the work and provided additional interpretations of the data collected in this study. All authors were involved in drafting this manuscript, final approval and accept accountability for all aspects of this work.

Acknowledgements

Special thanks goes to Oliver Tulloch and Roderick Read for their support and their excellent work in the theoretical and practical development of RAWES.

References

[1] Cherubini A, Papini A, Vertechy R and Fontana M 2015 Airborne Wind Energy Systems: A review of the technologies *Renewable and Sustainable Energy Reviews* **51** p 1461—1476
[2] Diehl M 2013 *Airborne Wind Energy* (Berlin: Springer) chapter 1 p 3–22
[3] Key de Souza Mendonça A, Vaz C R, Lezana A G R, Anacleto C A and Paladini E P 2017 Comparing Patent and Scientific Literature in Airborne Wind Energy *Sustainability* **9** p 1–22
[4] Read R 2018 *Airborne Wind Energy* Schmehl R (Singapor: Springer) chapter 12 p 515–37
[5] Tulloch O, Kazemi Amiri A, Yue H, Feuchtwang J and Read R, 2020 Tensile rotary power transmission model development for airborne wind energy systems *J. Phys.: Conf. Series* **1618** p 1–10
[6] Tulloch O 2021 *Modelling and Analysis of Rotary Airborne Wind Energy Systems* (Glasgow: Department of Electronic and Electrical Engineering University of Strathclyde)
[7] Webster G 2021 *The Kiteflier* **94** p 15–25

[8] Wacker J 2022 *Structural optimisation of airborne wind energy systems with rotary transmission* (Roskilde: DTU Wind Energy)
[9] Jonkman J M, Hayman G J, Jonkman B J, Damiani R R, Murray R E 2017 *AeroDyn v15 User's Guide and Theory Manual* (Denver: National Renewable Energy Laboratory)
[10] Beaupoil C 2019 *Practical experiences with a torsion based rigid blade Rotary Airborne Wind Energy System with ground based power generation* (Glasgow: Airborne Wind Energy Conference)
[11] Tulloch T, Read R and Tveide T 2019 *Book of Abstracts* (Milan: Airborne Wind Energy Conference)
[12] Shen W Z, Mikkelsen Rand Sørensen J N 2005 Tip loss corrections for wind turbine computations *Wind Energy* **8** p 457–75